Science of the Total Environment 848 (2022) 157840

Contents lists available at ScienceDirect

Science of the Total Environment

journal homepage: www.elsevier.com/locate/scitotenv

Nitrogen deposition increases xylem hydraulic sensitivity but decreases stomatal sensitivity to water potential in two temperate deciduous tree species

Da-Yong Fan [a,*], Qing-Lai Dang [b], Xiao-Fang Yang [c], Xiao-Ming Liu [c], Jia-Yi Wang [a], Shou-Ren Zhang [c,*]

[a] The Key Laboratory for Silviculture and Conservation of Ministry of Education, Beijing Forestry University, Beijing 100083, China
[b] Faculty of Natural Resources Management, Lakehead University, Thunder Bay, ON, Canada
[c] State Key Laboratory of Vegetation and Environmental Change, Institute of Botany, The Chinese Academy of Sciences, Beijing 100096, China

HIGHLIGHTS

- N deposition increased stomatal sensitivity to *VPD* for trees of *Quercus wutaishanica* and *Acer mono*.
- N deposition decreased stomatal sensitivity to water potential in both species.
- N deposition increased the vulnerability of the hydraulic system to cavitation in both species.
- N deposition would increase the risk of hydraulic failure in both species.

GRAPHICAL ABSTRACT

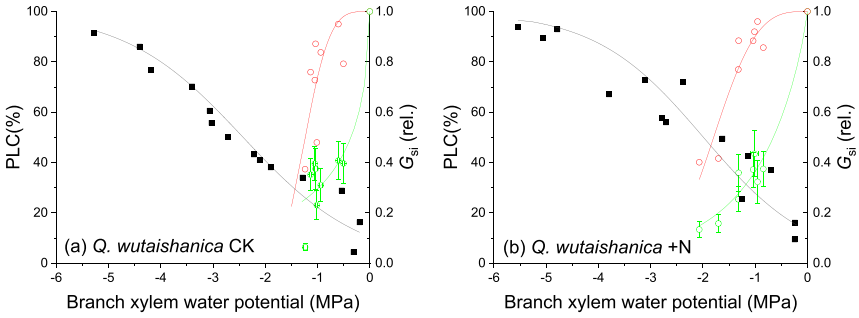

ARTICLE INFO

Editor: Zhaozhong Feng

Keywords:
Temperate forest
Nitrogen deposition
Water relations
Stomatal responses
Xylem embolism

ABSTRACT

Although the effects of nitrogen deposition on tree water relations are studied extensively, its impact on the relative sensitivities of stomatal and xylem hydraulic conductance to vapor pressure deficit and water potential is still poorly understood. This study investigated the effects of a 7-year N deposition treatment on the responses of leaf water relations and sensitivity of canopy stomatal conductance to vapor pressure deficit (*VPD*) and water potential, as well as the sensitivity of branch hydraulic conductance to water potential in a dominant tree species (*Quercus wutaishanica*) and an associated tree species (*Acer mono*) in a temperate forest. It was found that the N deposition increased stomatal sensitivity to *VPD*, decreased stomatal sensitivity to water potential, and increased the vulnerability of the hydraulic system to cavitation in both species. The standardized stomatal sensitivity to *VPD*, however, was not affected by the N deposition, indicating that the stomata maintained the ability to regulate the water balance under nitrogen deposition condition. Although the increased stomatal sensitivity to *VPD* could compensate the decreased stomatal sensitivity to water potential to some extent, the combined response would increase the percentage loss of hydraulic conductivity (PLC) when 50 % loss in stomatal conductance occurred, particularly in the dominant species *Q. wutaishanica*. The result indicates that N deposition would increase the risk of hydraulic failure in those species if the soil and/or air becomes drier under future climate change scenarios. The results of the study can have significant implications on the modelling of ecosystem vulnerability to drought under the scenario of atmospheric nitrogen deposition.

* Corresponding authors.
E-mail addresses: dayong73fan@163.com (D.-Y. Fan), zhangsrcn@hotmail.com (S.-R. Zhang).

http://dx.doi.org/10.1016/j.scitotenv.2022.157840
Received 25 May 2022Received in revised form 22 July 2022Accepted 1 August 2022
Available online xxxx

1. Introduction

Atmospheric N deposition has been increasing significantly due to increased fossil fuel combustion, urbanization and agriculture intensification (IPCC, 2007; Davidson, 2009). It is predicated that the N deposition rate will double the current rate by 2050 (Galloway et al., 2008). Increasing N availability in the soil can increase plant growth (Ripullone et al., 2004; Xia and Wan, 2008; Reay et al., 2008; Li et al., 2015; Schulte Uebbing and de Vries, 2017), and change hydraulic architecture (Borghetti et al., 2016), which in turn will impact plant water relations (Kleiner et al., 1992; Goldstein et al., 2013). Hydraulic adjustments in woody plants may influence their survival (Brodribb et al., 2020), ecosystem resistance and resilience (McGregor et al., 2021) to environmental stresses, particularly drought. Such resistance and resilience will become even more important to ecosystems as climate change has been increasing the frequency and severity of drought stress and drought (and heat)-related forest die-off (Allen et al., 2010; Choat et al., 2018; McDowell et al., 2020). Therefore, a good understanding of the long-term effects of N deposition on plant water relations is critical for improving the prediction of ecosystem responses to global change (Anderegg et al., 2016).

The current results on the effects of N deposition and its interaction with drought on the physiology and growth of forests are inconsistent and not well understood. N deposition may decrease plant survival during and after drought stress as it may increase limitations to photosynthesis and hydraulic failure (Gessler et al., 2017). Studies have showed that the hydraulic safety of branches (Zhang et al., 2021a, 2021b, 2021c) and leaves (Zhang et al., 2021a, 2021b, 2021c) have been compromised by nitrogen deposition, while the hydraulic conductance and stomatal conductance (Borghetti et al., 2016; Zhang et al., 2021a, 2021b, 2021c) are increased due to anatomical alterations (Bucci et al., 2006; Watanabe et al., 2008; Hacke et al., 2010; Plavcová and Hacke, 2012; Jiang et al., 2018). These studies suggest that the plant may face hydraulic failure if nitrogen deposition and drought stress increase further under the scenario of continued global climate change. In contrast, other studies have shown that nitrogen deposition can mitigate the effect of drought stress *via* improving carbon sequestration and reserves (Zhang et al., 2021a, 2021b, 2021c; Dulamsuren and Hauck, 2021). Furthermore, there are studies that have demonstrated that N deposition is neither a major nor a consistent driver of forest productivity responses to drought in European forest ecosystems (van der Graaf et al., 2021). Chronic N depositions to the soil can also reduce forest growth if the N concentration reaches or exceeds toxic levels (Aber et al., 1998; Li et al., 2013).

Stomatal sensitivity to changes in environmental conditions may be a contributor to the above conflicting results (Zhang et al., 2018). Stomates are the critical control of gas exchanges and water interactions between plants and the atmosphere (Buckley, 2019). The sensitivity and regulation of stomatal conductance influence tree growth and survival under drought conditions at both tree and ecosystem levels (McDowell et al., 2008, 2020). Stomata can respond to changes in soil and atmospheric moisture conditions *via* either a feedback (Oren et al., 1999) or feed-forward mechanism (Franks et al., 1997). The magnitude and rate of changes in stomatal conductance or aperture in response to environmental stimulus are, therefore, closely associated with hydraulic conductance and hydraulic sensitivity (Sperry et al., 2017; Anderegg et al., 2018). The relative sensitivities of stomatal conductance and xylem hydraulic conductance to water potential determine the risk of hydraulic failure under drought stress (Martínez Vilalta et al., 2014). Plants can maintain water homeostasis if stomatal conductance is more sensitive than hydraulic conductance to dry conditions. A consequence of high stomatal sensitivity to water potential is reduced carbon assimilation under dry conditions, which explains why isohydric pine species are less tolerant of long-term drought than anisohydric pine species (McDowell et al., 2008). Furthermore, soil or plant water potential and *VPD* can jointly affect stomatal sensitivity in the field (Jarvis, 1976; Dang et al., 1997; Leuschner et al., 2022). Although a meta-analysis has led to the hypothesis that nitrogen deposition reduces stomatal sensitivity to water potential (Zhang et al., 2018), there is no measured data to support it.

Lab and field measurements of stomatal response to water potential (stomatal vulnerability curve) indicate that 20 % loss of hydraulic conductivity due to xylem embolism has a functional association with 50 % loss in stomatal conductance in some tree species (Brodribb and Holbrook, 2003a, 2003b). However, measuring stomatal response to water potential in the field is complicated because of the high variability of *VPD* in the field which also has substantial impact on stomatal conductance. There are also complications with lab measurements because the chemical signals from roots and soil are excluded when the measurements are conducted on detached branches (Dang et al., 1997). An empirical model of the relationship between predawn and midday water potential may shed some light on the relative sensitivity of stomatal conductance and hydraulic conductance in the field (Martínez Vilalta et al., 2014). However, the effect of water potential on stomatal conductance is confounded with the effect of *VPD* in the model. The two effects need to be disentangled to better assess the risk of hydraulic failure to be imposed by N disposition in the future in the scenario of global climate change.

China is one of the three regions in the world with the highest rate of N deposition (Dentener, 2006). N deposition has increased by approximately 60 % over the past decades (Liu et al., 2013). The temperate broad-leaf forest in China is located in the area with the highest N deposition rate (Yu et al., 2019). N supply is a predominant limiting factor to plant growth in temperate regions (Vitousek and Howarth, 1991; Elser et al., 2007; Xing et al., 2022) and the deposition effect of N deposition can significantly affect the physiology and growth of plants in the region, including stomata behavior and hydraulic characteristics of plants. This study investigated the responses of canopy conductance, branch hydraulics, leaf water relations and stomatal sensitivity to water potential/*VPD* in a dominant tree species (*Quercus wutaishanica*) and an associated tree species (*Acer mono*) to N deposition in a temperate forest in China in a 7-year experiment. *Q. wutaishanica* is a dominant tree species in warm temperate deciduous broad-leaved forest area in China (Chen, 1997), while *A. mono* is a common deciduous tree widely distributed in northeastern Asia (van Gelderen, 1994). We tested the hypothesis that N deposition would increase the hydraulic efficiency by increasing the vessel diameter but would also increase the risk of hydraulic failure, according to the trade-off between hydraulic efficiency and safety. We further hypothesized that nitrogen deposition would reduce stomatal sensitivity to water potential but would increase its sensitivity to *VPD*.

2. Materials and methods

2.1. Study site

The experiments were conducted in an experimental area of the Beijing Forest Ecosystem Research Station of the Chinese Academy of Sciences located in the Dongling Mountain of Mentougou District of Beijing (39°57′ N, 115°25′E, and elevation 1296 m). It has a typical warm temperate continental monsoon climate with an average annual precipitation of 500–650 mm. The annual mean temperature is 7 °C, and the monthly mean temperatures of January and July are −7.8 °C and 21.1 °C, respectively. The temperate forest is dominated by oak (*Quercus wutaishanica*) and the associated tree species are primarily maple (*Acer mono*), ash (*Fraxinus rhynchophylla*) and birch (*Betula dahurica*). The canopy height of *Quercus wutaishanica* was 8–10 m and that of *Acer mono* was 3–8 m. The average stand density was 431 stems per hectare (Chen, 1997).

2.2. Nitrogen deposition treatment

The long-term nitrogen deposition experiment was established in 2013. There were four independent 15 m × 15 m fertilized plots and a control plot of the same size was established adjacent to each of the N deposition plot. Urea equivalent to 20 kg N ha^{-2} was applied once a month during the growing season (May–September) when rainfall was abundant in this area and no application occurred beyond the growing season. The N

application was in addition to the actual background N deposition in the study area (>50 kg N ha^{-2} a^{-1} reported by Yu et al., 2019).

2.3. Sap flow measurements

Sap-flow gauges were installed at breast height in the stems of sample trees (Granier, 1987). The installation and maintenance of the gauges were conducted according to the protocol given by the manufacturer (SF-G, Ecomatik, Germany). The gauges were installed on 9 *Quercus* and 7 *Acer* trees which were from the both plots of the nitrogen deposition and control (see Supplementary Table 1 for details). The sap flux density (sap-flow density per unit area of sapwood, J_s, g m^{-2} s^{-1}) of the individual trees was measured with Granier-type heat pulse sensors (SF-G, Ecomatik, Germany). All the gauges were installed on the north side of the tree stem in the outer 30 mm of the xylem at 1.3 m height and were insulated from solar radiation using a reflective shield. 30-min averages of sap-flow density were recorded with a data logger. However, for G_{si} (m s^{-1}, mean canopy stomatal conductance to water vapor) calculation, we used the hourly data because only hourly meteorological data [e.g. air temperature (T_A), air relative humidity (RH%)] were available from the field meteorological station about 1 km away from the study site. *VPD* was calculated from on T_A and RH% (Buck, 1981). J_s was calculated using an empirical formula developed by Granier and Bréda (1996):

$$J_s = 0.0331 \times \left(\frac{\Delta T_m - \Delta T}{\Delta T}\right)^{1.231} \quad (1)$$

where J_s has a unit of g m^{-2} s^{-1}. ΔT is the temperature difference between the upper and lower probe of the gauge when there is sap flow and ΔT_m is the temperature difference when there is no sapflow (night values).

2.4. Canopy-level stomatal conductance from sap flux measurement

We determined the canopy stomatal conductance for each sample tree from the sap flux measurements. Canopy transpiration E (g m^{-2} s^{-1}) was estimated according to Granier and Loustau (1994):

$$E = J_s * \text{Huber value} \quad (2)$$

where J_s (g m^{-2} s^{-1}) is the sap-flow density per unit of sapwood area and Huber value (m^2 m^{-2}) is the cross-section sapwood area per unit leaf area.

The terminal branch (at the same position as water potential and hydraulic conductance measurements) was used to estimate the Huber value of the tree. The difference between the Huber value determined from the measurement of the entire tree and that determined from the terminal shoot is generally <20 % (Jarvis, 1976; Margolis et al., 1995; Togashi et al., 2015; Lehnebach et al., 2018), and can be predicted by the pipe model theory (Shinozaki et al., 1964). Furthermore, the standardized stomatal sensitivity to *VPD* (m/b) is not affected by the variation of Huber value, as both m and b are calculated based on the same Huber value, where m is G_{si} sensitivity to *VPD*, and b is the stomatal conductance at 1 kPa *VPD*.

Branch sapwood cross-sectional area was determined by measuring the diameter of the acropetal end of each branch segment using a digital micrometer. Pith area was subtracted from gross cross-sectional area after measuring its dimension under a dissecting microscope equipped with a stage micrometer. Sample leaves were first scanned with a scanner (EPSON, Japan), and then the area of each was calculated using WinFOLIA software (Regent, Canada). The Huber value was calculated as the ratio of sapwood cross-sectional area to leaf area. At least nine replicates were used for each sample tree.

The sap-flux-scaled G_{si} was calculated using the following equation (Ewers and Oren, 2000; Monteith and Unsworth, 2013):

$$G_{si} = \frac{K_G(T_A)E}{VPD} \quad (3)$$

where $K_G(T_A)$ (kPa m^3 g^{-1}) is the conductance coefficient as a function of temperature [$= 115{,}800 + 422.6 \times T_A$ (°C)] (Ewers and Oren, 2000), which integrates the psychrometric constant, latent heat of vaporization, specific heat of air at constant pressure, and air density. The unit of G_{si} was then transformed from m s^{-1} to mmol m^{-2} s^{-1} according to Cowan and Farquhar (1977):

$$g_s\left(\frac{\text{mmol}}{\text{m}^2\text{s}}\right) \times 1000 = g_s\left(\frac{m}{s}\right)/100 \times 0.446 \times \left[\frac{273}{273+T}\right] \times \left[\frac{P}{101.3}\right] \quad (4)$$

where T is air temperature (°C), P is atmospheric pressure (KPa).

2.5. G_{si} sensitivity to VPD

The relationship between G_{si} and *VPD* is described using a modified Lohammar's function (Oren model):

$$G_{si} = -m \cdot \ln VPD + b \quad (5)$$

The G_{si} calculated from sap flux might suffer from the following uncertainties: 1) the diffusion of the transpiration signal by the depletion and replenishment of stem-stored water (Meinzer et al., 2009; Braun et al., 2010); 2) the irradiance effect on stomatal opening (Buckley and Mott, 2013); 3) the effect of leaf boundary layer conductance (*BLC*) (Ewers et al., 2005); 4) the effects of water potential and other environmental factors. Therefore, the canopy stomatal conductance at a specific *VPD* could be seriously underestimated and the reliability of Eq. (5) outputs is highly questionable. However, the maximum G_{si} based on sap flux at the similar *VPD* can only be used if the forementioned influences are minimized. Therefore, a boundary regression method on the flux-based G_{si} over consecutive days is better than the common regression over a single day (Mediavilla and Escudero, 2003). As such, we applied the quantile regression (QR) approach, fitted quantile regression models for the 90 % quantiles to describe the upper bound, and used sap flux density data of 35 days in the growing season of 2020. We only used sap flux density measurements from 0900 h to 1300 h for the analysis of G_{si} sensitivity to *VPD* to further minimize those effects. Matheny et al. (2015) demonstrate that the depletion of stored water in the stem occurs from 0800 h to 1800 h at a constant rate, and the replenishment occurs from 1800 h to 0800 h at a non-linear rate in oak and maple tree species during sunny days. Bunce (2000) has observed that when irradiance is higher than 500 μmol m^{-2} s^{-1}, stomatal conductance is quite stable in two crop species. Stomatal response to red light is related to photosynthesis (Buckley and Mott, 2013). Midday photoinhibition observed in the field generally leads to decreases in both photosynthesis and stomata conductance in afternoon. Therefore, the time period of 0900 h–1300 h provided a good time window to take measurements with minimal influence from the above effects.

2.6. Bench drying vulnerability curves

In August 2020, sunlit branches sampled from the upper canopy in both species were selected. The leafy end of branches of at least 2.0 m long for *Quercus wutaishanica* and at least 0.9 m long for *Acer mono* were sampled between 0530 and 0630 h, covered with a large black plastic bag with its cut submerged under water, and transported to an air-conditioned laboratory (25 °C). A preliminary test based on the method of Jacobsen et al. (2007) showed that the cutting length is more than twice the maximum vessel length of each species. To achieve a wide range of xylem tensions, some branches were air dried under dim light conditions (<10 μmol m^{-2} s^{-1} PAR) in the lab for periods of up to 6 h (until PLC >85 %) and then bagged for a minimum of 1 h to allow xylem pressure to equilibrate across the branch. After one hour equilibration time, branches were double-cut under water to relax residual tension, according to the protocol of Wheeler et al. (2013). The first cut was made more than the maximum length of one vessel from the end direction and the second cut was made one third of the maximum vessel length from the apical direction.

Following the cuts, the tension-relaxed branch segments (about 5–8 cm in length) in the middle of the remaining part were cut for the measurement of percentage loss of hydraulic conductivity (PLC, %). The flow rate through the segment was recorded using a XYL'EM apparatus (Bronkhorst, Montigny-les-Cormeilles, France). Filtered (0.2 μm) and degassed water containing 10 mM KCl was used to perfuse the samples. Native flow rate was recorded under low pressure (k_i, kg MPa^{-1} s^{-1}, 6 kPa). Maximum flow rate (k_m) was recorded under the same low hydrostatic pressure after air emboli was flushed out by perfusion under 130–150 kPa for 30 min. PLC was calculated as

$$PLC = 100 \times \frac{k_m - k_i}{k_m} \quad (6)$$

The specific hydraulic conductivity k_s (kg m^{-1} MPa^{-1} s^{-1}) was calculated by dividing k_m by the segment's cross-section sapwood area. For xylem pressure (Ψ, MPa) measurements, sampled leaves were sealed in aluminum to achieve equilibration before the measurement was taken using a Scholander pressure chamber (PMS Instrument, Corvallis, Oregon, USA). The branch hydraulic vulnerability curve for each sample was fitted with a cumulative Weibull function (Martínez Vilalta et al., 2014)

$$\frac{PLC}{100} = e^{-\left(\frac{\Psi}{c_k}\right)^{k_k}} \quad (7)$$

where c_k is the water potential at 63 % loss of the hydraulic conductivity and k_k is the slope of the vulnerability curve.

2.7. Midday and predawn water potential measurements

The predawn (Ψ_{dawn}, MPa, between 0530 and 0630 h) and midday water potential (Ψ_{min}, MPa, between 1200 and 1300 h) of branches were measured according to Pockman and Sperry (2000): a branch of similar size at the similar position to those used in the hydraulic vulnerability curve measurements was selected and sealed in a big black plastic bag containing a moist paper towel for 1 h in darkness to allow the equilibration of water potential between leaves and the subtending branch. Then the petiole water potential of a leaf was measured. The measurements were made on 8 different days (August 10th, 11th, 14th, 15th, and September 5th, 8th, 9th, 10th in 2020). There were at least 9 paired replicates for each species within each treatment. The midday and predawn branch water potential measurements were made on adjacent (paired) branches.

2.8. G_{si} sensitivity to Ψ

The averages of G_{si} measurements between 1200 h and 1300 h for each tree on each of the measurement days were used to investigate G_{si} sensitivity to midday Ψ. The sensitivity of stomatal conductance to water potential can be modeled empirically as 1 minus the corresponding cumulative Weibull function (Martínez Vilalta et al., 2014):

$$G_{si} = G_{simax} \times \left(1 - e^{-\left(\frac{\Psi}{c_g}\right)^{k_g}}\right) \quad (8)$$

where c_g is the water potential at 63 % loss of stomatal conductance; k_g is the slope of the G_{si} *vs.* Ψ curve. G_{simax} was obtained from the maximum G_{si} recorded in 35 days in the growing season.

Under uncontrolled environmental conditions in the field, stomata not only respond to Ψ, but also to other factors such as *VPD*, irradiance, CO_2 concentration and temperature (Jarvis, 1976). Although in the current situation (at noon in the eight sunny and sunny-cloudy days within one month), irradiance, CO_2 concentration and temperature (Supplementary Table 2) were similar across different days, *VPD* could greatly affect the analysis of G_{si} sensitivity to Ψ. Therefore, we replaced G_{simax} with a realistic maximum G_{si} at a specific *VPD*, as described by Eq. (5) if the interactive effect of *VPD* and Ψ is not taken into account for simplicity. We also applied the multiplicative constraint model (Ogle and Reynolds, 2002) to

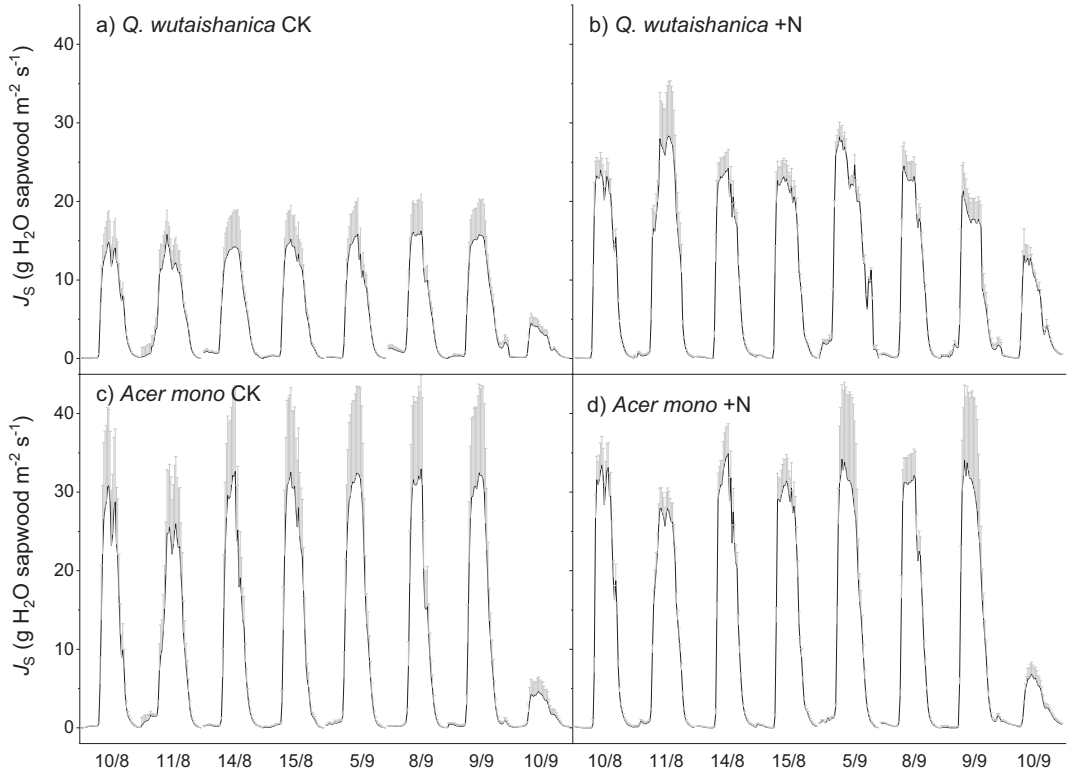

Fig. 1. Daily sap flux density (+s.e.) of *Quercus wutaishanica* and *Acer mono* in response to nitrogen deposition on the 8 measurement days. Values were calculated using Eqs. (1) and (2) (see text for details).

investigate if *VPD* values at noon in the eight days were larger than $e^{-\frac{b-G_{simax}}{m}}$ for each species and treatment. The fact that all were lower than the threshold indicates that Eq. (5) is robust. As such, the real stomatal sensitivity to water potential can be modified as:

$$G_{si} = G_{simax\_real} \times \left(1 - e^{-\left(\frac{\Psi}{c_{greal}}\right)^{k_{greal}}}\right) \quad (9)$$

where $G_{simax\text{-}real}$ was calculated based on Eq. (5), c_{greal} is the real water potential at 63 % loss of stomatal conductance; k_{greal} is the slope of the corresponding G_{si} *vs.* Ψ curve.

2.9. Foliar carbon isotope discrimination

After the measurement of Huber value, leaves distal to the measured samples were oven-dried at 70 °C for 48 h and finely ground. A subsample of 1 mg of ground leaf was combusted and analyzed for ^{13}C-^{12}C composition using an isotope ratio mass spectrometer (EA-DELTA plus XP, Thermo Fisher Scientific, USA). Leaf carbon isotope composition ($\delta^{13}C$) was calculated as:

$$\delta^{13}C = \frac{R_{sa} - R_{st}}{R_{st}} \times 1000 \quad (10)$$

where R_{sa} and R_{st} are the $^{13}C/^{12}C$ ratio in the sample and in the conventional Pee Dee Belemnite standard, respectively.

2.10. Statistical analyses

The distribution normality of hydraulic traits were tested by calculating the Shapiro-Wilk W statistics. Differences between treatments were tested using Kruskal-Wallis H test if $P(W) < 0.05$, and ANOVA if $P(W) > 0.05$. Non-linear regression model with the *gnls* () function of R software was applied to bench drying vulnerability curves and G_{si}-to-Ψ sensitivity curves. The QR was carried out by using the 'quantreg' packages in R (Koenker et al., 2018). We conducted all the statistical analyses using R version 4.0.5 (R Development Core, 2017).

3. Results

Variations in the 30-min average sap flow of the 16 sample trees on each measurement day (August 10th, 11th, 14th, 15th, and September 5th, 8th, 9th, 10th in 2020) are shown in Fig. 1. In the control plots, J_s of *A. mono* was generally larger than that of *Q. wutaishanica*. In 7 out of the 8 measurement days, maximum J_s values were 31.4 ± 0.9 (s.e.) g H_2O m^{-2} s^{-1} for *A. mono* and 15.4 ± 0.3 g H_2O m^{-2} s^{-1} for *Q. wutaishanica*. Nitrogen deposition significantly increased the average maximum J_s of *Q. wutaishanica*, to 24.8 ± 1.0 g H_2O m^{-2} s^{-1}. The N deposition also increased J_s of *A. mono*, but the effect was less obvious (32.5 ± 0.9 by the N deposition). However, the sap flow density on September 10th was much lower than those on other measurement days for both species and in both treatments because it was a dry day with a *VPD* as high as 2.41 kPa at 1300 h.

Fig. 2 demonstrated the relationship between G_{si} and *VPD* of representative trees at 0900, 1000, 1100, 1200, 1300 h of 35 consecutive days in the growth season in 2020. There were 175 data points in total for each species and treatment, and the upper boundary of the data could be fitted very

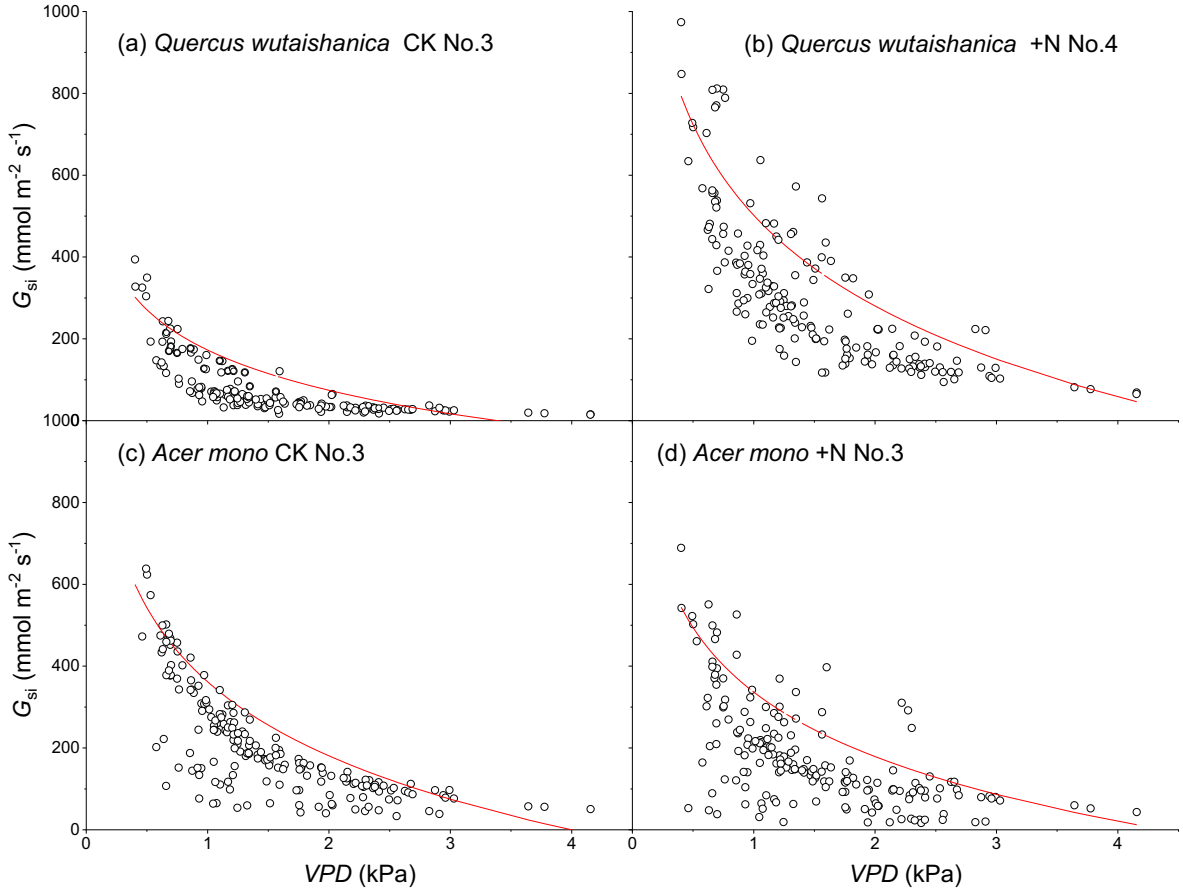

Fig. 2. G_{si} response to *VPD* from 175 measurements taken at 0900, 1000, 1100, 1200 and 1300 h on 35 days. 90 % Quantile Regression method was applied to obtain *m* and *b* values (red lines). "No." means the number of the tree for sap flow measurement, see Supplementary Table 1 for details.

Table 1
Means and standard error of G_{simax} (mmol $m^{-2} s^{-1}$), m (mmol $m^{-2} s^{-1}$ ln (kPa)$^{-1}$), b (mmol $m^{-2} s^{-1}$) and m/b for *Quercus wutaishanica* and *Acer mono* in N deposition treatment (+N) and control (CK). Treatment and species combinations labeled with different letters were significantly different from each other ($P \leq 0.05$).[a]

Species & treatment		G_{simax}	m	b	m/b
Q. wutaishanica CK		387 ± 68^{b}	121 ± 24^{b}	171 ± 37^{b}	0.71 ± 0.05^{a}
Q. wutaishanica + N		1075 ± 205^{a}	276 ± 61^{a}	418 ± 86^{a}	0.65 ± 0.02^{a}
Acer mono CK		677 ± 195^{ab}	234 ± 52^{ab}	361 ± 73^{ab}	0.65 ± 0.03^{a}
Acer mono + N		784 ± 55^{ab}	255 ± 20^{ab}	364 ± 33^{ab}	0.70 ± 0.03^{a}
P value	Species(S)	0.74	0.60	0.62	0.71
	Treatment (T)	0.02*	0.066	0.051	0.66
	S * T	0.10	0.15	0.09	0.14

[a] *: $P < 0.05$.

Table 2
Means and standard error for k_s (kg m^{-1} MPa^{-1} s^{-1}), Huber value ($\times 10^{-4}$ m^2 m^{-2}), $\delta^{13}C$ (‰) of *Quercus wutaishanica* and *Acer mono* in N deposition treatment (+N) and control (CK). Treatment and species combinations labeled with different letters were significantly different[a] from each other ($P \leq 0.05$). Nitrogen deposition.

Species & treatment		k_s	Huber value	$\delta^{13}C$
Q. wutaishanica CK		2.51 ± 0.10^{b}	1.42 ± 0.22^{b}	−27.89 ± 0.37^{a}
Q. wutaishanica + N		3.11 ± 0.25^{a}	2.14 ± 0.25^{a}	−27.68 ± 0.30^{a}
Acer mono CK		0.44 ± 0.02^{c}	1.12 ± 0.15^{b}	−29.50 ± 0.21^{b}
Acer mono + N		0.51 ± 0.02^{c}	1.30 ± 0.15^{b}	−29.11 ± 0.15^{b}
P value	Species(S)	<0.001***	0.009**	0.002**
	Treatment (T)	0.04*	0.03*	0.70
	S * T	0.17	0.21	0.40

[a] *: $P < 0.05$, **: $P < 0.01$, ***: $P < 0.001$.

well by the Eq. (5) (all $R^2 > 0.98$, $P < 0.01$). The maximum stomatal canopy conductance (G_{simax}) was generally higher in *A. mono* (577 mmol $m^{-2} s^{-1}$) than in *Q. wutaishanica* (387 mmol $m^{-2} s^{-1}$), but the difference was not statistically significant (Table 1). The N deposition significantly increased G_{simax} of both species ($P = 0.02$), particularly for *Q. wutaishanica* which increased by about three times. The N deposition increased both G_{si} sensitivity to *VPD* (m) and the reference G_{si} at 1 kPa (b) in both *Q. wutaishanica* and *A. mono* but the magnitude of increase was greater in *Q. wutaishanica* than in *A. mono*. The m and b values of *Q. wutaishanica* increased by 128 %, and 144 % respectively, while those of *A. mono* increased by 9 % and 1 %. However, there was no significant impact on the standardized G_{si} sensitivity to *VPD* (m/b) in the two species (Table 1; Fig. 3).

The specific hydraulic conductivity (k_s) of branches in *Q. wutaishanica* was about six times higher than that of *A. mono* (Table 2). The N deposition increased k_s of both species, particularly for *Q. wutaishanica* (by 24 %, $P < 0.05$), and by 16 % ($P > 0.05$) for *A. mono*. *Q. wutaishanica* had a higher Huber value than *A. mono*. The N deposition also increased Huber value of both species, particularly for *Q. wutaishanica* (by 51 %, $P < 0.05$). $\delta^{13}C$ of *Q. wutaishanica* was significantly higher than that *A. mono* ($P < 0.05$), but the N deposition did not significantly affect $\delta^{13}C$ in the two species.

The N deposition significantly influenced the relationship between Ψ_{dawn} and Ψ_{min} in the two species (Fig. 4): In *Q. wutaishanica*, the deposition increased the slope of the relationship by 87 %, but did not significantly affect the intercept of the regression ($P > 0.05$); In *A. mono*, the deposition increased the slope and also decreased the intercept, but neither effect was statistically significant ($P > 0.05$).

The nitrogen deposition increased the hydraulic sensitivity to water potential in both species (Fig. 5). For example, Ψ_{50} (water potential at 50 % PLC) in control and fertilized *Q. wutaishanica* were −2.42 and −1.92 MPa, respectively; Ψ_{50} for control and fertilized *A. mono* were −2.50 and −2.09 MPa, respectively. Ψ_{63} (c_k, water potential corresponding to 63 % PLC) for unfertilized and fertilized *Q. wutaishanica* were −3.15 MPa and −2.52 MPa, respectively; Ψ_{63} for unfertilized and fertilized *A. mono* were −3.13 MPa and −2.59 MPa, respectively. The N deposition decreased k_k from 1.14 to 0.93 in *Q. wutaishanica* and from 1.00 to 0.99 in *A. mono*. In contrast, the nitrogen deposition decreased G_{si} sensitivity to Ψ in both species (Fig. 5). In *Q. wutaishanica*, the deposition decreased c_g (the water potential corresponding to 63 % loss of stomatal conductance) from −0.70 MPa to −0.99 MPa and increased k_g from 0.55 to 0.88; In *A. mono*, the deposition decreased c_g from −1.00 MPa to −1.07 MPa and decreased k_g from 1.97 to 1.02.

The shape of the cumulative Weibull curve of G_{si} sensitivity to Ψ changed substantially when *VPD* effect was excluded. For example, the real c_{greal} decreased to −1.35 MPa as compared to an empirical c_g of −0.70 MPa for *Q. wutaishanica* CK, −2.01 MPa compared to −0.99 MPa for *Q. wutaishanica* + N, −1.10 compared to −1.00 MPa for *Acer mono* CK, and −1.73 MPa compared to −1.07 MPa for *Acer mono* + N, respectively (Fig. 5). The results further confirmed the nitrogen deposition decreased G_{si} sensitivity to Ψ in both species.

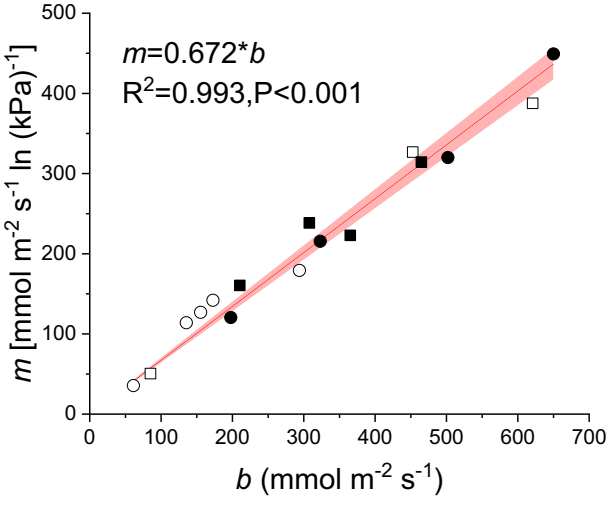

Fig. 3. Relationship between m and b in *Quercus wutaishanica* (circle) and *Acer mono* in N fertilized treatment (solid square) and control (empty square). The slope was significant different from 0.6 (95 % LCL = 0.642, 95 % UCL = 0.701). Red band represents the 95 % confidence interval of linear regression line.

4. Discussion

4.1. Effects of nitrogen deposition on stomatal sensitivity to VPD

The nitrogen deposition increased maximum G_{si} and stomatal sensitivity to *VPD* (m) significantly in *Q. wutaishanica* but non-significantly in *A. mono*. A higher maximum stomatal conductance generally is associated with a higher stomatal sensitivity to *VPD*, particularly in mesic woody species (Oren et al., 1999; Katul et al., 2009). The results are in line with the conclusions of two meta-analyses (Zhang et al., 2018; Liang et al., 2020). Nitrogen depositions generally lead to higher leaf nitrogen concentration, larger stomates and higher rates of photosynthesis (Zhu et al., 2020), particularly in upper canopy trees exposed to higher PAR (photosynthetic active radiation). Indeed, the G_{simax} and m in the upper canopy of *Q. wutaishanica* responded to the deposition to much greater extents than the lower canopy tree species, *A. mono*.

The present study showed that nitrogen deposition did not change the standardized stomatal sensitivity to *VPD* (m/b), indicating that the species were capable of regulating stomatal conductance to maintain relatively stable water relations even when there was a significant amount of nitrogen deposition in the soil. To our knowledge, this is the first study in the literature investigating the effect of nitrogen deposition on m/b. The stomatal sensitivity to *VPD* in *Q. wutaishanica* in the control treatment is similar to

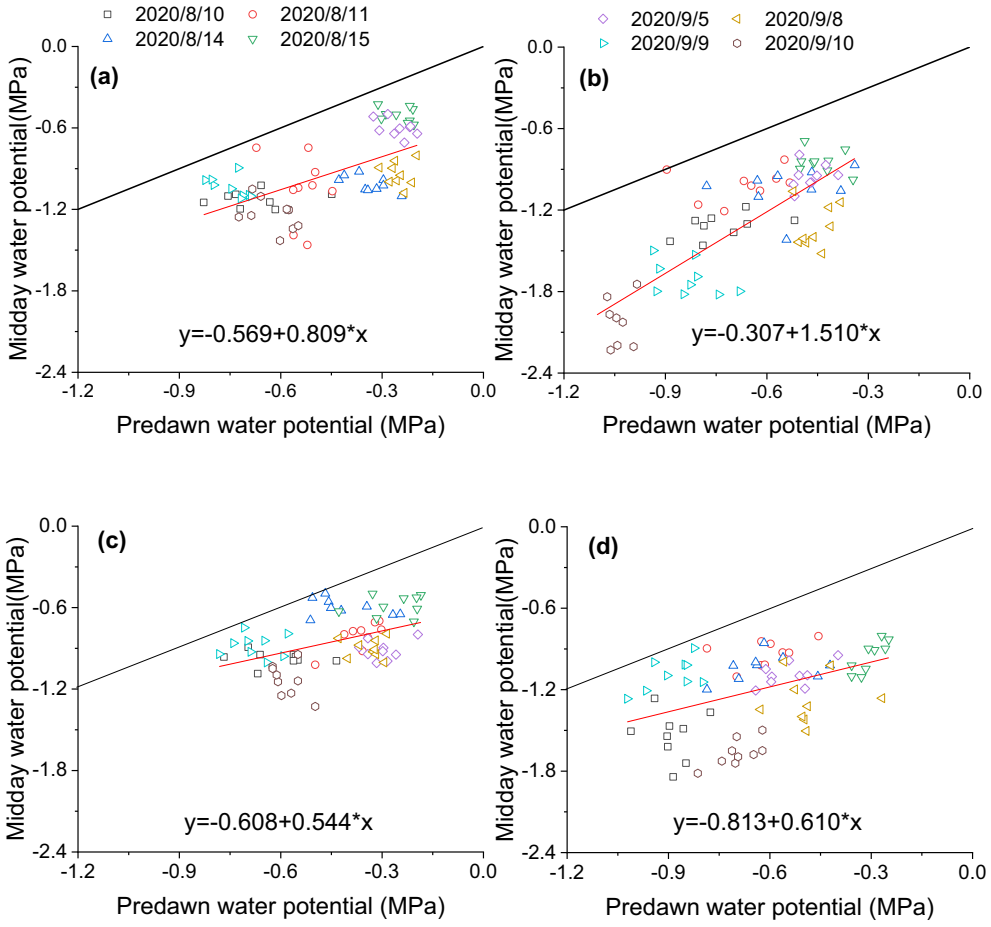

Fig. 4. Relationship between predawn and midday leaf water potentials for *Quercus wutaishanica* and *Acer mono*. (a) *Q. wutaishanica* (CK): *F*, *P* and R^2 for the linear regression were 45.249, <0.001 and 0.384, respectively; 95 % CI range was −0.449 to −0.689 for the intercept and 0.569 to 1.049 for the slope. (b). *Q. wutaishanica* (+N): *F*, *P* and R^2 were 117.913, <0.001 and 0.627, respectively. The 95 % CI range for intercept, slope were (−0.118, −0.496), and (1.232, 1.787) respectively. (c). *A. mono* (CK): *F*, *P* and R^2 were 19.003, <0.001 and 0.202, respectively; 95 % CI range was −0.726 to −0.491 for intercept and 0.295 to 0.795 for the slope. (d). *A. mono* (+N): *F*, *P* and R^2 were 16.437, <0.001 and 0.179, respectively; 95 % CI range −1.012 to −0.615 for intercept and 0.310 to 0.911 for slope. Black lines represented 1:1 lines, and red lines were the linear regression fits.

the value reported for *Q. alba* grown at a lowland site (Phillips et al., 1996). Numerous other studies have demonstrated that the standardized stomatal sensitivity to *VPD* (*m*/*b*) of C3 plants converges at 0.6 under various environmental conditions, such as different CO_2 concentrations (Maherali et al., 2003), different groundwater depths (Fan et al., 2020), different growing-season temperatures (Poyatos et al., 2007), different light regimes (Tarvainen et al., 2013), and in species of different climate origins (Bourne et al., 2015). This conclusion is consistent with the theoretical expectations of a hydraulic model for stomatal regulation where stomatal conductance is regulated to maintain relatively stable rates of transpiration and leaf water potential. However, *m*/*b* in this study converged to 0.67, slightly above the value of 0.60 in the literature for mesic species (Oren et al., 1999).

Canopy conductance determined from sap flux tends to show similar trends to those shown by leaf area-based conductance (Oren et al., 1999; Addington et al., 2004). It can be argued that the G_{si} is autocorrelated with *VPD* because *VPD* is also used in the calculation of G_{si} (Monteith, 1995). However, using an alternative method to calculate G_{si} did not change the shape of the relationship between *VPD* and G_{si} (Monteith, 1995; Oren et al., 1999). In fact, *b* is the stomatal conductance at 1 kPa *VPD* which often occurs in field measurements. The reference canopy stomatal conductances (*b*) of the two species are in agreement with values of leaf scale conductance in the literature (Hanba et al., 2002; Lin et al., 2002; Nabeshima and Hiura, 2004; Liu et al., 2019), indicating the canopy conductance derived from sap flux measurements is comparable to values of leaf scale conductance reported by similar studies.

VPD as the major driving force of transpiration was generally below 3 kPa during the growing season in the study area (Fig. 2). The Oren model has shown that the slope of the conductance sensitivity curve (*m*/*b*) can increase to 0.68 for the *VPD* range of 1–3 kPa, very close to the value found in this study. Furthermore, the Oren model predicts that the *m*/*b* value is constant only if stomata conductance is regulated perfectly to maintain relative constant transpiration and leaf water potential, which is the case of *A. mono* in this study (Fig. 4c & d). However, the nitrogen deposition obviously increased the range of diurnal variation in tissue water potential of *Q. wutaishanica*, which showed a clear transition from isohydric behavior to anisohydric behavior as defined by Meinzer et al. (2016) in response to the nitrogen deposition (Fig. 4a & b). This discrepancy can be reconciled by modifying the Oren model by relaxing the constant water potential assumption and when both the tight relationship between leaf specific hydraulic conductance (k_l) and G_{si} (Addington et al., 2004; Broddrib and Holbrook, 2003a) and the regulation of k_l *via* xylem cavitation or changes in conductance of non-xylem tissue (Scoffoni et al., 2017) are taken into account. The results using the Oren model with relaxed assumption have demonstrated that plants can regulate k_l under variable $\Delta\Psi$ (water potential differential between soil and leaf) conditions to maintain *m*/*b* constant (Fan et al., 2020; Ranawana et al., 2021).

Stomatal sensitivity to *VPD* is tightly related to water-use efficiency (Franks and Farquhar, 1999) and may be coordinated with photosynthesis (Aphalo and Jarvis, 1993; Damour et al., 2010). The stable carbon isotope composition $\delta^{13}C$ is an indicator of long-term integrated water use

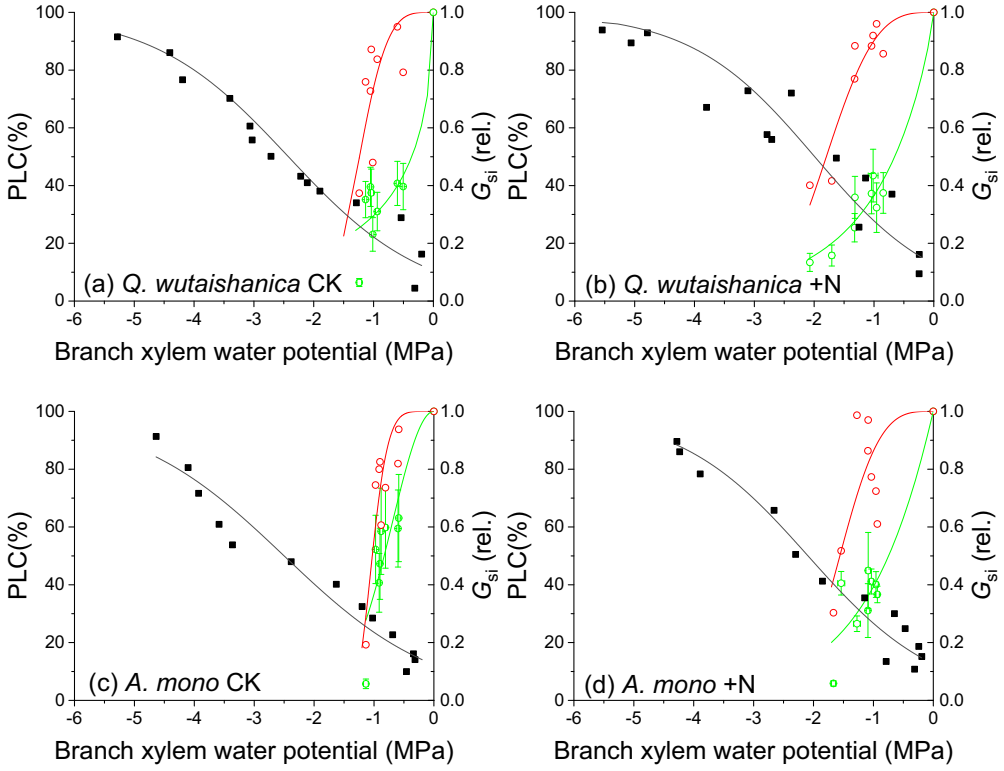

Fig. 5. Vulnerability to embolism curves generated by bench top dehydration method, apparent stomatal sensitivity and real stomatal sensitivity to water potential for *Quercus wutaishanica* and *Acer mono* in N deposition treatment (+N) and control (CK). Solid squares and black lines represent PLC data points generated using bench drying methods and the corresponding hydraulic vulnerability curves, respectively. Green circles and lines represent apparent G_{si} sensitivity to Ψ and the corresponding stomata "vulnerability" curves. Red circles and lines represent the real G_{si} sensitivity to Ψ and the corresponding stomata "vulnerability" curves. Bar: +s.e. Because the real G_{si} was obtained by the Eq. (4), and the relative G_{si} was calculated as the ratio between real G_{si} and G_{simax}, there was no s.e. for red circles.

efficiency and was not significantly affected by the nitrogen deposition in either of the two species in this study (Table 2), which is consistent with the findings of other studies on the same ecosystem (Zhu et al., 2019; Liu et al., 2019) and the conclusion of a meta-analysis (Zhang et al., 2018; Liang et al., 2020). The $\delta^{13}C$ results further corroborate our finding that the N deposition had no significant effect on the standardized stomatal sensitivity to *VPD* (*m/b*). It is interesting to note that *A. mono* had significantly lower $\delta^{13}C$ than *Q. wutaishanica*, which is in contrast to the finding of Liu et al. (2019) that there is no significant difference in instantaneous photosynthetic water use efficiency between the two species, possibly due to the interspecific variation in the draw-down of CO_2 from the intercellular spaces to the chloroplast as regulated by the mesophyll resistance (Flexas and Ribas-Carbo, 2008).

4.2. Effects of N deposition on stomatal and hydraulic sensitivities to water potential

The nitrogen deposition significantly increased the branch Ψ_{50} in both species. The result indicates that the fertilized trees suffered xylem cavitation or embolism at less negative water potentials than their unfertilized counterparts, making them less resistant to drought stress. The nitrogen deposition increased the xylem hydraulic vulnerability by 20.7 % in *Q. wutaishanica* and 16.4 % in *A. mono*. Furthermore, the N deposition increased c_k (water potential at 63 % PLC) and decreased k_k (slope of the xylem VC curve) in both species. Our results are consistent with the finding of a meta-analysis that nitrogen deposition increases Ψ_{50} by an average of 21.5 % across tree species in different biomes (Zhang et al., 2018). Therefore, both our study and the meta-analysis suggest that nitrogen deposition will likely increase the risk of hydraulic failure, particularly if the soil and air become drier with continued changes in the climate, unless stomates become more sensitive and better able to control water loss.

The decreased resistance of branch xylem hydraulic system to more negative water potential by the nitrogen deposition as indicated by the increases in k_s suggests a trade-off between hydraulic safety and hydraulic efficiency within a species. Such a trade-off is also reported for other species (Gleason et al., 2016). The intra-specific trade-off indicates a structural regulation (Lovelock et al., 2006). The hydraulic conductivity of a conduit is positively related to the fourth power of its diameter based on the Hagen-Poiseuille equation (Tyree and Zimmermann, 2013). However, larger-diameter conduits tend to be more vulnerable to cavitation, particularly freeze-thaw induced cavitation (Choat et al., 2003). The nitrogen deposition in this study increased the vessel diameter of *Q. wutaishanica* by 22.08 %, and that of *A. mono* by 7.68 % without changing vessel density (data not shown), indicating *Q. wutaishanica* showed more pronounced trade-off between efficiency and safety than *A. mono*. These results suggest that *Q. wutaishanica* will probably benefit more from nitrogen deposition than *A. mono* under non-drought conditions but will be at a higher risk of hydraulic failure if drought becomes more severe in the future. Our results are consistent with the findings of other studies in the same ecosystem (Zhang et al., 2021a).

The xylem hydraulic system is only one of the factors influencing the water relations and vulnerability of plants to cavitation. Therefore, the increase in xylem vulnerability to water deficit that induced cavitation does not necessarily mean an increasing risk of hydraulic failure as some studies suggest (Gessler et al., 2017; Zhang et al., 2018; Liang et al., 2020). A corresponding increase in stomatal sensitivity to water potential can compensate for or off-set the increase in the sensitivity of the hydraulic transport system to avoid catastrophic hydraulic failure from "run-away" cavitations (Tyree and Sperry, 1988). The relative sensitivities of stomatal conductance and hydraulic conductance to soil water availability can be empirically quantified by the slope (σ) of the relationship between predawn water potential and midday water potential (Martínez Vilalta et al., 2014). This

slope increased significantly in *Q. wutaishanica* in response to the nitrogen deposition in this study (Fig. 4), suggesting that hydraulic conductance declined faster than stomatal conductance did when water potential declined. However, it should be pointed out that the response of stomatal conductance to water potential could have been confounded with its response to *VPD* or the interaction between *VPD* and water potential because we were unable to hold *VPD* constant during the measurements.

To disentangle the above confounding effects, we firstly investigated the apparent response of G_{si} to water potential in the field. The nitrogen deposition decreased c_g (water potential at 63 % loss of stomatal conductance), which is the opposite to the response of the xylem hydraulic system. Furthermore, the N deposition decreased the water potential threshold for 50 % stomatal closure in both species, particularly for *Q. wutaishanica* (from −0.70 MPa to −0.99 MPa). The water potential at 50 % stomatal closure induced a PLC of 14 % in *Q. wutaishanica* CK, and 21 % in *A. mono* CK. However, the shape of stomatal "vulnerable curve" as obtained in the present study is quite different from that by Brodribb & Holbrook, 2003a, 2003b: their curves are generally "S" shaped, *i.e.*, stomatal conductance is stable at high water potentials, drops quickly as water potential declines further, and become stable again when the water potential becomes really low, whereas ours are "L" shaped, *i.e.*, stomatal conductance decreased quickly with decreasing water potential for the entire range of the measured water potential (Fig. 5). The "L" shaped curves could also occur in the field (McDowell et al., 2008; Bartlett et al., 2016). It is postulated that the "L" shaped curves in the present study were probably caused by the larger variability of *VPD*, as the air temperature and irradiance conditions were comparable in our 8 days of mid-day (1200 to 1300 h) measurements (Supplementary Table 2). We used Eq. (5) to exclude the *VPD* effect to obtain the sole effect of water potential on stomatal conductance in the field.

As expected, the shape of stomatal "vulnerability curve" returned to "S"-like shape after *VPD* effect was excluded (Fig. 5). This contradicts the previous argument that the "L" shaped curves reflect the true water potential responses. The water potential at 50 % stomatal closure induced 26 % PLC in *Q. wutaishanica* CK, and 23 % in *A. mono* CK, compared with 14 % and 21 % when *VPD* was included, which are close to the value of ≈20 % reported by others (Brodribb & Holbrook, 2003a, 2003b). This result also suggests that there was no strong vulnerability segmentation in the two species (Brodribb and Holbrook, 2003a). Interestingly, the N deposition increased PLC from 26 % to 45 % at 50 % stomatal closure in *Q. wutaishanica*, and from 23 % to 38 % in *A. mono*. Furthermore, the N deposition decreased c_{greal} (the real water potential at which 63 % of stomatal conductance is lost) and k_{greal} (the curve was less steep). All the results confirm that the nitrogen deposition decreased the sensitivity of stomata to water potential. As such, the results do not support the inter-specific finding that species with more vulnerable xylem tend to be completely compensated by having even more sensitive stomata (Nardini and Salleo, 2000; Martínez Vilalta et al., 2014). Indeed, the nitrogen deposition could induce more sensitive stomata to evaporative demand (m), which can compensate less sensitive stomata to upstream hydraulic supply (c_{greal}), to prevent the occurrence of massive xylem cavitation to some extents. This could be inferred from the fact that PLC could drop from 45 % (sole effect by water potential on stomata response) to 21 % (a mixed effect by water potential and *VPD* on stomata response) at 50 % stomatal closure in *Q. wutaishanica*, and from 38 % to 22 % in *A. mono*.

The more sluggish stomatal response to water potential in the fertilized trees indicates a lower bulk turgor loss point (Ψ_{TLP}). Ψ_{TLP} is a key indicator of stomatal response (Brodribb and Holbrook, 2003a) although it should be used with caution (Farrell et al., 2017; Buckley, 2019). Lower Ψ_{TLP} values are also reported in nitrogen-fertilized trees grown in water-limited areas (Fang et al., 2018). There are also studies reporting opposite results, *i.e.*, nitrogen deposition increases Ψ_{TLP} (Tan and Hogan, 1997) or has no effect on Ψ_{TLP} (Jin et al., 2020). Therefore, further investigations are warranted on the response of Ψ_{TLP} to nitrogen deposition, particularly on the mechanisms of the response. However, the mechanism of increases in stomatal sensitivity to *VPD* seems more certain and is primarily attributed to increases in peristomatal transpiration for a higher G_{si} as driven by a specific *VPD*, and may also be related to changes in anatomy induced by increases in nitrogen supply (Mott and Parkhurst, 1991; Bucci et al., 2006; Watanabe et al., 2008; Hacke et al., 2010; Plavcová and Hacke, 2012; Jiang et al., 2018). The changes in G_{simax} and stomatal sensitivity to water potential and *VPD* may have contributed to the higher photosynthesis rates and faster growth in the fertilized trees of both species (data not shown). The IPCC2007 (Solomon et al., 2007) projects a robust pattern of increased precipitation in North Temperate Zone, to the end of the 21st century. If the prediction becomes true, the changes in G_{simax} and stomatal sensitivity to water potential and *VPD* will be beneficial to those trees. However, the number of dry days are also predicted to increase in many places, including the study area (Pörtner et al., 2022). These tendencies arise from the reduction in the frequency of precipitation, the increases in precipitation intensity and runoff, and the increases in evapotranspiration (Trenberth, 2011). As such, nitrogen deposition may increase the risk of hydraulic failure for both species as indicated by the 14 % to 21 % increases in PLC in *Q. wutaishanica* and 21 % to 22 % PLC increases in *A. mono* accompanied by a 50 % stomatal closure. Further, the dominant tree species, *Q. wutaishanica*, is likely to be more vulnerable to drought.

5. Conclusions

Although the effect of soil nitrogen deposition on tree water relations has been studied extensively (*e.g.*, Xia and Wan, 2008; Zhang et al., 2018; Liang et al., 2020), there is a paucity of data on the relative sensitivities of stomatal conductance and xylem hydraulic conductivity to water potential. We found that the nitrogen deposition increased the relative sensitivity of the xylem hydraulic system but reduced the relative sensitivity of stomatal conductance to water potential in both species. The nitrogen deposition also increased stomatal sensitivity to *VPD*. However, the nitrogen treatment did not affect the values of standardized stomatal sensitivity to *VPD*. The increase in stomatal sensitivity to *VPD* did not fully compensate for the effect of decreases in stomatal sensitivity to water potential by the nitrogen deposition, leading to increases in percentage loss of xylem hydraulic conductance at the water potential with 50 % loss of stomatal conductance, particularly in the canopy species *Q. wutaishanica*. The results indicate that the risk of hydraulic failure in the ecosystem may increase if the soil and/or air becomes drier and soil N increases under the predicted future climate change conditions. The results of the study can have significant implications on the modelling of ecosystem vulnerability to drought under the scenario of atmospheric nitrogen deposition.

Funding sources

The support of this work by the National Key Research and Development Program of China (2016YFA0600802) is gratefully acknowledged.

CRediT authorship contribution statement

Da-Yong Fan: Conceptualization, Data curation, Formal analysis, Investigation, Methodology, Resources, Software, Validation, Visualization, Writing – original draft, Writing – review & editing.

Qing-Lai Dang: Conceptualization, Methodology, Resources, Supervision, Validation, Visualization, Writing-review & editing.

Xiao-Fang Yang: Data curation, Methodology, Visualization, Writing – review & editing.

Xiao-Ming Liu: Data curation, Methodology, Writing – review & editing.

Jia-Yi Wang: Data curation, Methodology, Writing – review & editing.

Shou-Ren Zhang: Conceptualization, Data curation, Investigation, Methodology, Funding acquisition, Project administration, Writing – review & editing.

Data availability

Data will be made available on request.

Declaration of competing interest

Neither author has any conflict of interest.

Appendix A. Supplementary data

Supplementary data to this article can be found online at https://doi.org/10.1016/j.scitotenv.2022.157840.

References

Aber, J., McDowell, W., Nadelhoffer, K., Magill, A., Berntson, G., Kamakea, M., McNulty, S., Currie, W., Rustad, L., Fernandez, I., 1998. Nitrogen saturation in temperate forest ecosystems: hypotheses revisited. Bioscience 48, 921–934.

Addington, R.N., Mitchell, R.J., Oren, R., Donovan, L.A., 2004. Stomatal sensitivity to vapor pressure deficit and its relationship to hydraulic conductance in pinus palustris. Tree Physiol. 24, 561–569.

Allen, C.D., Macalady, A.K., Chenchouni, H., Bachelet, D., Mcdowell, N., Vennetier, M., 2010. A global overview of drought and heat-induced tree mortality reveals emerging climate change risks for forests. For. Ecol. Manag. 259, 660–684.

Anderegg, W.R.L., Klein, T., Bartlett, M., Sack, L., Pellegrini, A.F.A., Choat, B., Jansen, S., 2016. Meta-analysis reveals that hydraulic traits explain cross-species patterns of drought-induced tree mortality across the globe. PNAS 113, 5024–5029.

Anderegg, W.R.L., Wolf, A., Arango Velez, A., Choat, B., Chmura, D.J., Jansen, S., Kolb, T., Li, S., Meinzer, F.C., Pita, P., 2018. Woody plants optimise stomatal behaviour relative to hydraulic risk. Ecol. Lett. 21, 968–977.

Aphalo, P.J., Jarvis, P.G., 1993. An analysis of Ball's empirical model of stomatal conductance. Ann. Bot. 72, 321–327.

Bartlett, M.K., Klein, T., Jansen, S., Choat, B., Sack, L., 2016. The correlations and sequence of plant stomatal, hydraulic, and wilting responses to drought. PNAS 113, 13098–13103.

Borghetti, M., Gentilesca, T., Leonardi, S., Noije, T., Rita, A., 2016. Long-term temporal relationships between environmental conditions and xylem functional traits: a meta-analysis across a range of woody species along climatic and nitrogen deposition gradients. Tree Physiol. 37, 4–17.

Bourne, A.E., Haigh, A.M., Ellsworth, D.S., 2015. Stomatal sensitivity to vapour pressure deficit relates to climate of origin in eucalyptus species. Tree Physiol. 35, 266–278.

Braun, S., Schindler, C., Leuzinger, S., 2010. Use of sap flow measurements to validate stomatal functions for mature beech (Fagus Sylvatica) in view of ozone uptake calculations. Environ. Pollut. 158, 2954–2963.

Brodribb, T.J., Powers, J., Cochard, H., Choat, B., 2020. Hanging by a thread? Forests and drought. Science 368, 261–266.

Brodribb, T., Holbrook, N.M., 2003a. Relations between stomatal closure, leaf turgor and xylem vulnerability in eight tropical dry forest trees. Plant Cell Environ. 26, 443–450.

Brodribb, T.J., Holbrook, N.M., 2003b. Stomatal closure during leaf dehydration, correlation with other leaf physiological traits. Plant Physiol. 132, 2166–2173.

Bucci, S.J., Scholz, F.G., Goldstein, G., Meinzer, F.C., Franco, A.C., Campanello, P.I., Villalobos-Vega, R., Bustamante, M., Miralles-Wilhelm, F., 2006. Nutrient availability constrains the hydraulic architecture and water relations of Savannah trees. Plant Cell Environ. 29, 2153–2167.

Buck, A., 1981. New equations for computing vapor pressure and enhancement factor. J. Appl. Meteorol. Climatol. 20, 1527–1532.

Buckley, T.N., 2019. How do stomata respond to water status? New. Phytol. 224, 21–36.

Buckley, T.N., Mott, K.A., 2013. Modelling stomatal conductance in response to environmental factors. Plant Cell Environ. 36, 1691–1699.

Bunce, J.A., 2000. Responses of stomatal conductance to light, humidity and temperature in winter wheat and barley grown at three concentrations of carbon dioxide in the field. Glob. Chang. Biol. 6, 371–382.

Chen, L.Z., 1997. The importance of Donglin Mountain region of warm temperate deciduous broad-leaved forest. In: Chen, L.Z. (Ed.), The Study on Structure and Function of Forest in Warm Temperate Zone. Science Press, Beijing, pp. 1–9.

Choat, B., Ball, M., Luly, J., Holtum, J., 2003. Pit membrane porosity and water stress-induced cavitation in four co-existing dry rainforest tree species. Plant Physiol. 131, 41–48.

Choat, B., Brodribb, T.J., Brodersen, C.R., Duursma, R.A., López, R., Medlyn, B.E., 2018. Triggers of tree mortality under drought. Nature 558, 531–539.

Cowan, I.R., Farquhar, G.D., 1977. Stomatal function in relation to leaf metabolism and environment. Symp. Soc. Exp. Biol. 31, 471–505.

Damour, G., Simonneau, T., Cochard, H., Urban, L., 2010. An overview of models of stomatal conductance at the leaf level. Plant Cell Environ. 33, 1419–1438.

Dang, Q.L., Margolis, H.A., Coyea, M.R., Sy, M., Collatz, G.J., 1997. Regulation of branch-level gas exchange of boreal trees: roles of shoot water potential and vapour pressure difference. Tree Physiol. 17, 521–535.

Davidson, E.A., 2009. The contribution of manure and fertilizer nitrogen to atmospheric nitrous oxide since 1860. Nat. Geosci. 2, 659–662.

Dentener, F.J., 2006. Global Maps of Atmospheric Nitrogen Deposition, 1860, 1993, and 2050. ORNL DAAC.

Dulamsuren, C., Hauck, M., 2021. Drought stress mitigation by nitrogen in boreal forests inferred from stable isotopes. Glob. Chang. Biol. 27, 5211–5224.

Elser, J.J., Bracken, M.E.S., Cleland, E.E., Gruner, D.S., Harpole, W.S., Hillebrand, H., Ngai, J.T., Seabloom, E.W., Shurin, J.B., Smith, J.E., 2007. Global analysis of nitrogen and phosphorus limitation of primary producers in freshwater, marine and terrestrial ecosystems. Ecol. Lett. 10, 1135–1142.

Ewers, B.E., Oren, R., 2000. Analyses of assumptions and errors in the calculation of stomatal conductance from sap flux measurements. Tree Physiol. 20, 579–589.

Ewers, B.E., Gower, S.T., Bond Lamberty, B., Wang, C.K., 2005. Effects of stand age and tree species on canopy transpiration and average stomatal conductance of boreal forests. Plant Cell Environ. 28, 660–678.

Fan, D.Y., Dang, Q.L., Xu, C.Y., Jiang, C.D., Zhang, W.F., Xu, X.W., Yang, X.F., Zhang, S.R., 2020. Stomatal sensitivity to vapor pressure deficit and the loss of hydraulic conductivity are coordinated in Populus euphratica, a desert phreatophyte species. Front. Plant Sci. 11, 1248.

Fang, L., Zhao, Q., Liu, Y., Hao, G., 2018. The influence of a five-year nitrogen fertilization treatment on hydraulic architecture of Pinus sylvestris var. mongolica in a water-limited plantation of NE China. For. Ecol. Manag. 418, 15–22.

Farrell, C., Szota, C., Arndt, S.K., 2017. Does the turgor loss point characterize drought response in dryland plants? Plant Cell Environ. 40, 1500–1511.

Flexas, J., Ribas-Carbo, M., 2008. Mesophyll conductance to CO2: current knowledge and future prospects. Plant Cell Environ. 31, 602–621.

Franks, P.J., Farquhar, G.D., 1999. A relationship between humidity response, growth form and photosynthetic operating point in C3 plants. Plant Cell Environ. 22, 1337–1349.

Franks, P.J., Cowan, I.R., Farquhar, G.D., 1997. The apparent feedforward response of stomata to air vapour pressure deficit: information revealed by different experimental procedures with two rainforest trees. Plant Cell Environ. 20, 142–145.

Galloway, J.N., Townsend, A.R., Erisman, J.W., Bekunda, M., 2008. Transformation of the nitrogen cycle: recent trends, questions and potential solutions. Science 320, 889–892.

Gessler, A., Schaub, M., McDowell, N.G., 2017. The role of nutrients in drought-induced tree mortality and recovery. New Phytol. 214, 513–520.

Gleason, S.M., Westoby, M., Jansen, S., Choat, B., Hacke, U.G., Pratt, R.B., Bhaskar, R., Brodribb, T.J., 2016. Weak tradeoff between xylem safety and xylem-specific hydraulic efficiency across the world's woody plant species. New Phytol. 209, 123–136.

Goldstein, G., Bucci, S.J., Scholz, F.G., 2013. Why do trees adjust water relations and hydraulic architecture in response to nutrient availability? Tree Physiol. 33, 238–240.

Granier, A., 1987. Evaluation of transpiration in a Douglas-fir stand by means of sap flow measurements. Tree Physiol. 3, 309–320.

Granier, A., Bréda, N., 1996. Modelling canopy conductance and stand transpiration of an oak forest from sap flow measurements. Ann. Sci. For. 53, 537–546.

Granier, A., Loustau, D., 1994. Measuring and modelling the transpiration of a maritime pine canopy from sap-flow data. Agric. For. Meteorol. 71, 61–81.

Hacke, U.G., Plavcova, L., Almeida-Rodriguez, A., King-Jones, S., Zhou, W., Cooke, J.E.K., 2010. Influence of nitrogen fertilization on xylem traits and aquaporin expression in stems of hybrid poplar. Tree Physiol. 30, 1016–1025.

Hanba, Y.T., Kogami, H., Terashima, I., 2002. The effect of growth irradiance on leaf anatomy and photosynthesis in acer species differing in light demand. Plant Cell Environ. 25, 1021–1030.

IPCC (Intergovernmental Panel on Climate Change), 2007. Climate Change 2007: The Scientific Basis. Cambridge University Press, New York, NY, USA.

Jacobsen, A.L., Pratt, R.B., Davis, S.D., Ewers, F.W., 2007. Cavitation resistance and seasonal hydraulics differ among three arid californian plant communities. Plant Cell Environ. 30, 1599–1609.

Jarvis, P., 1976. The interpretation of the variations in leaf water potential and stomatal conductance found in canopies in the field. Philos. Trans. R. Soc. Lond. 273, 593–610.

Jiang, X., Liu, N., Lu, X., Huang, J., Cheng, J., Guo, X., Wu, S., 2018. Canopy and understory nitrogen deposition increase the xylem tracheid size of dominant broadleaf species in a subtropical forest of China. Sci. Total Environ. 642, 733–741.

Jin, Y., Wang, C., Zhou, Z., Gu, J., 2020. Contrasting responses of hydraulic traits between leaf and branch to 16-year nitrogen deposition in a larch plantation. For. Ecol. Manag. 475, 118461.

Katul, G.G., Palmroth, S., Oren, R., 2009. Leaf stomatal responses to vapour pressure deficit under current and CO2 -enriched atmosphere explained by the economics of gas exchange. Plant Cell Environ. 32, 968–979.

Kleiner, K.W., Abrams, M.D., Schultz, J.C., 1992. The impact of water and nutrient deficiencies on the growth, gas exchange and water relations of red oak and chestnut oak. Tree Physiol. 11, 271–287.

Koenker, R., Portnoy, S., Ng, P., Zeileis, A., Grosjean, P., Ripley, B., 2018. Quantreg: Quantile Regression, Version 5.3. 4. R Package.

Lehnebach, R., Beyer, R., Letort, V., Heuret, P., 2018. The pipe model theory half a century on: a review. Ann. Bot. 121, 773–795.

Leuschner, C., Schipka, F., Backes, K., 2022. Stomatal regulation and water potential variation in European beech: challenging the iso/anisohydry concept. Tree Physiol. 42, 365–378.

Li, J.L., Dang, Q.L., Man, R.Z., Marfo, J., 2013. Elevated CO2 alters N- growth relationship in spruce and causes unequal increases in N, P and K demands. For. Ecol. Manag. 298, 19–26.

Li, W., Guan, D., Wang, A., 2015. The effects of simulated nitrogen deposition on plant root traits: a meta-analysis. Soil Biol. Biochem. 82, 112–118.

Liang, X., Zhang, T., Lu, X., Ellsworth, D.S., Bassirirad, H., You, C., Wang, D., He, P., Deng, Q., Liu, H., Mo, J., Ye, Q., 2020. Global response patterns of plant photosynthesis to nitrogen deposition: a meta-analysis. Glob. Chang. Biol. 26, 3585–3600.

Lin, C., Ma, Q., Han, H., Cao, W., Wang, Z., Wang, B., 2002. Photosynthesis characteristic of Quercus liaotungensis in Taiyue Mountain region. Acta Ecol. Sin. 22, 1399–1406.

Liu, X., Zhang, Y., Han, W., Tang, A., Shen, J., Cui, Z., Vitousek, P., Erisman, J.W., Goulding, K., Christie, P., Fangmeier, A., 2013. Enhanced nitrogen deposition over China. Nature 494, 459–462.

Liu, X.M., Yang, X.F., Wang, X., Zhang, S.R., 2019. Effects of simulated nitrogen deposition on growth and photosynthetic characteristics of Quercus wutaishanica and Acer pictum subsp. mono in a warm-temperate deciduous broad-leaved forest. Chin.J. Ecol. 43, 197–207.

Lovelock, C.E., Ball, M.C., Choat, B., Engelbrecht, B.M., Holbrook, N.M., Feller, I.C., 2006. Linking physiological processes with mangrove forest structure: phosphorus deficiency

limits canopy development, hydraulic conductivity and photosynthetic carbon gain in dwarf Rhizophora mangle. Plant Cell Environ. 29, 793–802.
Maherali, H., Johnson, H.B., Jackson, R.B., 2003. Stomatal sensitivity to vapour pressure difference over a subambient to elevated CO2 gradient in a C3/C4 grassland. Plant Cell Environ. 26, 1297–1306.
Margolis, H., Oren, R., Whitehead, D., Kaufmann, M.R., 1995. Leaf area dynamics of conifer forests. Ecophysiology of Coniferous Forests. Academic Press, pp. 181–223.
Martínez Vilalta, J., Poyatos, R., Aguadé, D., Retana, J., Mencuccini, M., 2014. A new look at water transport regulation in plants. New Phytol. 204, 105–115.
Matheny, A.M., Bohrer, G., Garrity, S.R., Morin, T.H., Howard, C.J., Vogel, C.S., 2015. Observations of stem water storage in trees of opposing hydraulic strategies. Ecosphere 6, 1–13.
McDowell, N., Pockman, W.T., Allen, C.D., 2008. Mechanisms of plant survival and mortality during drought: why do some plants survive while others succumb to drought? New Phytol. 178, 719–739.
McDowell, N.G., Allen, C.D., Anderson-Teixeira, K., Aukema, B.H., Bond-Lamberty, B., Chini, L., Clark, J.S., Dietze, M., Grossiord, C., Hanbury-Brown, A., Hurtt, G.C., 2020. Pervasive shifts in forest dynamics in a changing world. Science 368, eaaz9463.
Mcgregor, I.R., Helcoski, R., Kunert, N., Tepley, A.J., Gonzalez Akre, E.B., Herrmann, V., Zailaa, J., Stovall, A.E.L., Bourg, N.A., Mcshea, W.J., Pederson, N., Sack, L., Anderson Teixeira, K.J., 2021. Tree height and leaf drought tolerance traits shape growth responses across droughts in a temperate broadleaf forest. New Phytol. 231, 601–616.
Mediavilla, S., Escudero, A., 2003. Stomatal responses to drought at a Mediterranean site: a comparative study of co-occurring woody species differing in leaf longevity. Tree Physiol. 23, 987–996.
Meinzer, F.C., Johnson, D.M., Lachenbruch, B., Mcculloh, K.A., Woodruff, D.R., 2009. Xylem hydraulic safety margins in woody plants: coordination of stomatal control of xylem tension with hydraulic capacitance. Funct. Ecol. 23, 922–930.
Meinzer, F.C., Woodruff, D.R., Marias, D.E., Smith, D.D., Mcculloh, K.A., Howard, A.R., Magedman, A.L., 2016. Mapping 'hydroscapes' along the iso to anisohydric continuum of stomatal regulation of plant water status. Ecol. Lett. 19, 1343–1352.
Monteith, J., Unsworth, M., 2013. Principles of Environmental Physics: Plants, Animals, and the Atmosphere. Academic Press.
Monteith, J.L., 1995. A reinterpretation of stomatal responses to humidity. Plant Cell Environ. 18, 357–364.
Mott, K.A., Parkhurst, D.F., 1991. Stomatal responses to humidity in air and helox. Plant Cell Environ. 14, 509–515.
Nabeshima, E., Hiura, T., 2004. Size dependency of photosynthetic water- and nitrogen-use efficiency and hydraulic limitation in acer mono. Tree Physiol. 24, 745–752.
Nardini, A., Salleo, S., 2000. Limitation of stomatal conductance by hydraulic traits: sensing or preventing xylem cavitation? Tree Physiol. 15, 14–24.
Ogle, K., Reynolds, J.F., 2002. Desert dogma revisited: coupling of stomatal conductance and photosynthesis in the desert shrub, Larrea tridentata. Plant Cell Environ. 25, 909–921.
Oren, R., Sperry, J.S., Katul, G.G., Pataki, D.E., 1999. Survey and synthesis of intra-and interspecific variation in stomatal sensitivity to vapour pressure deficit. Plant Cell Environ. 22, 1515–1526.
Phillips, N., Oren, R., Zimmermann, R., 1996. Radial patterns of xylem sap flow in non-, diffuse- and ring-porous tree species. Plant Cell Environ. 19, 983–990.
Plavcová, L., Hacke, U.G., 2012. Phenotypic and developmental plasticity of xylem in hybrid poplar saplings subjected to experimental drought, nitrogen fertilization, and shading. J. Exp. Bot. 63, 6481–6491.
Pockman, W.T., Sperry, J.S., 2000. Vulnerability to xylem cavitation and the distribution of Sonoran Desert vegetation. Am. J. Bot. 87, 1287–1299.
Pörtner, H.O., Roberts, D.C., Adams, H., Adler, C., Aldunce, P., Ali, E., Begum, R.A., Betts, R., Kerr, R.B., Biesbroek, R., Birkmann, J., 2022. Climate change 2022: impacts, adaptation and vulnerability. AvailableContribution of Working Group II to the Sixth Assessment Report of the Intergovernmental Panel on Climate Change. Cambridge University Press . https://www.ipcc.ch/report/ar6/wg2/.
Poyatos, R., Martinez-Vilalta, J., Cermak, J., 2007. Plasticity in hydraulic architecture of Scots pine across Eurasia. Oecologia 153, 245–259.
R Development Core, T.collab, 2017. A Language and Environment for Statistical Computing.
Ranawana, S., Siddique, K.H.M., Palta, J.A., 2021. Stomata coordinate with plant hydraulics to regulate transpiration response to vapour pressure deficit in wheat. Funct. Plant Biol. 48, 839–850.
Reay, D.S., Dentener, F., Smith, P., Grace, J., Feely, R.A., 2008. Global nitrogen deposition and carbon sinks. Nat. Geosci. 1, 430–437.
Ripullone, F., Lauteri, M., Grassi, G., Amato, M., Borghetti, M., 2004. Variation in nitrogen supply changes water-use efficiency of Pseudotsuga menziesii and Populus X euroamericana; a comparison of three approaches to determine water-use efficiency. Tree Physiol. 24, 671–679.
Schulte Uebbing, L., Vries de, W., 2017. Global-scale impacts of nitrogen deposition on tree carbon sequestration in tropical, temperate, and boreal forests: a meta-analysis. Glob. Chang. Biol. 24, e416–e431.
Scoffoni, C., Albuquerque, C., Brodersen, C.R., Townes, S.V., John, G.P., Bartlett, M.K., Buckley, T.N., Mcelrone, A.J., Sack, L., 2017. Outside-xylem vulnerability, not xylem embolism, controls leaf hydraulic decline during dehydration. Plant Physiol. 173, 1197–1210.
Shinozaki, K., Yoda, K., Hozumi, K., Kira, T., 1964. A quantitative analysis of plant form-the pipe model theory: I.Basic analyses. Jpn. J. Ecol. 14, 97–105.
Solomon, S., Manning, M., Marquis, M., Qin, D., 2007. Climate Change 2007-The Physical Science Basis: Working Group I Contribution to the Fourth Assessment Report of the IPCC. vol. 4. Cambridge University Press.
Sperry, J.S., Venturas, M.D., Anderegg, W.R.L., Mencuccini, M., Mackay, D.S., Wang, Y., Love, D.M., 2017. Predicting stomatal responses to the environment from the optimization of photosynthetic gain and hydraulic cost. Plant Cell Environ. 40, 816–830.
Tan, W., Hogan, G.D., 1997. Physiological and morphological responses to nitrogen limitation in jack pine seedlings: potential implications for drought tolerance. New For. 14, 19–31.
Tarvainen, L., Wallin, G., Rantfors, M., Udding, J., 2013. Weak vertical canopy gradients of photosynthetic capacities and stomatal responses in a fertile Norway spruce stand. Oecologia 173, 1179–1189.
Togashi, H.F., Prentice, I.C., Evans, B.J., Forrester, D.I., Drake, P., Feikema, P., Brooksbank, K., Eamus, D., Taylor, D., 2015. Morphological and moisture availability controls of the leaf area Brooksbank, K., Eamus, D.pacities and stomatnts on Australian trees. Ecol.Evol. 5, 1263–1270.
Trenberth, K.E., 2011. Changes in precipitation with climate change. Clim. Res. 47, 123–138.
Tyree, M.T., Sperry, J.S., 1988. Do Woody plants operate near the point of catastrophic xylem dysfunction caused by dynamic water stress? 1: answers from a model. Plant Physiol. 88, 574–580.
Tyree, M.T., Zimmermann, M.H., 2013. Xylem Structure and the Ascent of Sap. Springer Science & Business Media.
van der Graaf, S.C., Janssen, T.A.J., Erisman, J.W., Schaap, M., 2021. Nitrogen deposition shows no consistent negative nor positive effect on the response of forest productivity to drought across European FLUXNET forest sites. Environ. Res. 3, 125003.
van Gelderen, D.M., 1994. Maple species and infraspecific taxa. In: van Gelderen, D.M., De Jong, P.C., Oterdoom, H.J. (Eds.), Maples of the World. Timber Press, Portland, OR, USA, pp. 105–240.
Vitousek, P.M., Howarth, R.W.J.B., 1991. Nitrogen limitation on land and in the sea: how can it occur? Biogeochemistry 13, 87–115.
Watanabe, Y., Tobita, H., Kitao, M., 2008. Effects of elevated CO2 and nitrogen on wood structure related to water transport in seedlings of two deciduous broad-leaved tree species. Trees 22, 403–411.
Wheeler, J.K., Huggett, B.A., Tofte, A.N., Rockwell, F.E., Holbrook, N.M., 2013. Cutting xylem under tension or supersaturated with gas can generate PLC and the appearance of rapid recovery from embolism. Plant Cell Environ. 36, 1938–1949.
Xia, J., Wan, S., 2008. Global response patterns of terrestrial plant species to nitrogen deposition. New Phytol. 179, 428–439.
Xing, A., Du, E., Shen, H., Xu, L., Vries, W., Zhao, M., Liu, X., Fang, J., 2022. Nonlinear responses of ecosystem carbon fluxes to nitrogen deposition in an old-growth boreal forest. Ecol. Lett. 25, 77–88.
Yu, G., Jia, Y., He, N., Zhu, J., Chen, Z., Wang, Q., Piao, S., Liu, X., He, H., Guo, X., Wen, Z., 2019. Stabilization of atmospheric nitrogen deposition in China over the past decade. Nat. Geosci. 12, 424–429.
Zhang, H., Li, W., Adams, H.D., Wang, A., Wu, J., Jin, C., Guan, D., Yuan, F., 2018. Responses of woody plant functional traits to nitrogen deposition: a meta-analysis of leaf economics, gas exchange, and hydraulic traits. Front. Plant Sci. 9, 683.
Zhang, H., Li, X., Guan, D., Wang, A., Yuan, F., Wu, J., 2021. Nitrogen nutrition deposition mitigated drought stress by improving carbon exchange and reserves among two temperate trees. Agric. For. Meteorol. 311, 108693.
Zhang, H., Yuan, F., Wu, J., Jin, C., Pivovaroff, A.L., Tian, J., Li, W., Guan, D., Wang, A., McDowell, N.G., 2021. Responses of functional traits to seven-year nitrogen deposition in two tree species: coordination of hydraulics, gas exchange and carbon reserves. Tree Physiol. 41, 190–205.
Zhang, T., Liang, X., BassiriRad, H., Liu, H., 2021. Leaf hydraulic acclimation to nitrogen deposition of two dominant tree species in a subtropical forest. Sci. Total Environ. 771, 145415.
Zhu, K., Wang, A., Wu, J., Yuan, F., Guan, D., Jin, C., Zhang, Y., Gong, C., 2020. Effects of nitrogen depositions on mesophyll and stomatal conductance in manchurian ash and mongolian oak. Sci. Rep. 10, 1–10.
Zhu, L., Hu, Y., Zhao, X., Zhao, P., 2019. Specific responses of sap flux and leaf functional traits to simulated canopy and understory nitrogen depositions in a deciduous broadleaf forest. Funct. Plant Biol. 46, 986–993.